Formation of highly hygroscopic soot aerosols upon internal mixing with sulfuric acid vapor

Khalizov, Alexei F.; Zhang, Renyi; Zhang, Dan; Xue, Huaxin; Pagels, Joakim; McMurry, Peter H.

Published in:
Journal of Geophysical Research

DOI:
10.1029/2008JD010595

2009

Formation of highly hygroscopic soot aerosols upon internal mixing with sulfuric acid vapor

Alexei F. Khalizov,[1] Renyi Zhang,[1] Dan Zhang,[1] Huaxin Xue,[1]
Joakim Pagels,[2,3] and Peter H. McMurry[2]

Received 12 June 2008; revised 25 November 2008; accepted 10 December 2008; published 7 March 2009.

[1] The hygroscopic properties of submicron soot particles during internal mixing with gaseous sulfuric acid have been investigated using a combined tandem differential mobility analyzer (TDMA) and differential mobility analyzer–aerosol particle mass analyzer (DMA-APM) technique. Fresh particles exhibit no change in mobility size and mass at subsaturated conditions, whereas particles exposed to gaseous sulfuric acid (10^9–10^{10} molecule cm^{-3}, 12 s contact time) experience significant mobility size and mass changes with increasing relative humidity (RH). The DMA-APM measurements reveal that particles of all sizes exposed to H_2SO_4 vapor gain mass with increasing RH because of absorption of water by sulfuric acid coating. However, on the basis of mobility size measurements using TDMA, upon humidification H_2SO_4-coated soot agglomerates display distinct hygroscopic growth patterns depending on their initial size and the mass fraction of condensed sulfuric acid. While small particles experience an increase in their mobility sizes, larger particles exhibit a marked shrinkage due to compaction. We suggest that determination of the hygroscopic properties of soot particles using a TDMA alone can be inconclusive. Restructuring of the soot agglomerates and filling of the voids that accompany the condensation of water-soluble materials and subsequent water absorption lead to little or no observable changes in particle mobility size at subsaturated RH even for particles that contain aqueous coatings. Extrapolation of our experimental results to the urban atmosphere indicates that initially hydrophobic soot particles acquire sufficient sulfate coating to become efficient CCN (cloud condensation nuclei) within a time period ranging from a few hours to a few days, dependent on the ambient H_2SO_4 level. The results imply that internal mixing with sulfuric acid through H_2SO_4 vapor condensation likely represents a common aging process for a variety of atmospheric aerosols. The variations in the size and hygroscopicity of soot particles during atmospheric processing influence their optical properties, cloud-forming potential, and human health effects.

Citation: Khalizov, A. F., R. Zhang, D. Zhang, H. Xue, J. Pagels, and P. H. McMurry (2009), Formation of highly hygroscopic soot aerosols upon internal mixing with sulfuric acid vapor, *J. Geophys. Res.*, *114*, D05208, doi:10.1029/2008JD010595.

1. Introduction

[2] Significant quantities of carbon soot aerosols are emitted into the atmosphere from a variety of anthropogenic and natural sources, including incomplete combustion of fossil fuels, biomass burning, and forest fires. Soot is an efficient light absorber in the visible and infrared spectral ranges and directly impacts the radiative balance of the Earth-atmosphere system by absorbing solar and terrestrial radiation [*Horvath*, 1993; *Jacobson*, 2001; *Li et al.*, 2005]. Fresh soot particles produced in the laboratory are typically hydrophobic and activate to cloud droplets only at supersaturations exceeding 10–20% [*Kotzick et al.*, 1997; *Zuberi et al.*, 2005]. Soot particles from atmospheric sources, such as jet and diesel engines, may contain a small fraction of water-soluble material, which makes them slightly hygroscopic [*Hitzenberger et al.*, 2003]. The soluble fraction increases because of aging and the aged soot particles may become efficient cloud condensation nuclei (CCN) and ice nuclei (IN), modifying the microphysical and the radiative properties and lifetime of clouds [*Andreae and Rosenfeld*, 2008; *Fan et al.*, 2008]. Soot aging includes adsorption and condensation of semivolatile vapors, coagulation with preexisting aerosol particles, heterogeneous reactions with atmospheric gaseous species, and cloud processing. These processes occur directly at the source, such as the internal mixing of soot with unburned organics and sulfuric acid in diesel and jet engine exhaust [*Weingartner et al.*, 1997; *Gysel et al.*, 2003; *Sakurai et al.*, 2003a; *Olfert et al.*, 2007] and water-soluble ash, such as KCl and K_2SO_4 [*Rissler et al.*, 2005], or take place during soot transport in the atmosphere

[1]Department of Atmospheric Sciences, Texas A&M University, College Station, Texas, USA.
[2]Department of Mechanical Engineering, University of Minnesota, Minneapolis, Minnesota, USA.
[3]Division of Ergonomics and Aerosol Technology, Faculty of Engineering, Lund University, Sweden.

0148-0227/09/2008JD010595

[*Saathoff et al.*, 2003; *Shiraiwa et al.*, 2007; *Moteki et al.*, 2007; *Shi et al.*, 2008]. While coating of the combustion particles with sulfuric acid increases their hygroscopicity, the presence of low-volatile organic compounds formed at lower combustion temperatures partially compensates the hygroscopic effect of sulfuric acid [*Petzold et al.*, 2005]. The change in hygroscopicity of soot particles during aging has an important influence on their atmospheric residence time, optical properties, and cloud-forming potential [*Andreae and Rosenfeld*, 2008]. Aging also influences the chemical reactivity of soot aerosols. It has been shown that hydrophobic soot chemically reduces NO_2 to HONO [*Ammann et al.*, 1998; *Aubin and Abbatt*, 2007], while hydrophilic soot oxidizes NO_2 via aqueous-phase reactions in adsorbed water [*Gundel et al.*, 1989].

[3] Freshly generated soot exists in the form of chain-like or compact aggregates composed of hydrophobic spherical primary particles with diameters typically ranging from 10 to 50 nm. Previous work has suggested that the irregular geometry and complex microstructure of the soot aggregates provide possible active sites for water condensation [*Crouzet and Marlow*, 1995]. This was experimentally supported by *Weingartner et al.* [1997] who observed shrinking and restructuring of highly agglomerated soot particles produced in a spark discharge generator and exposed to elevated relative humidity (RH) approaching water saturation. Because of the inverse Kelvin effect, enough water condenses in small angle cavities of the particles so that the resulting capillary forces cause the branches of agglomerates to partially collapse. However, the amount of water that physically adsorbs on fresh soot is insufficient to activate the fresh soot particles into cloud droplets under atmospherically relevant critical supersaturations [*Kotzick et al.*, 1997; *Zuberi et al.*, 2005]. In contrast, after exposure to oxidizing environments of nitric acid, ozone, and OH radicals, aged soot particles reversibly absorb large amounts of water and activate at significantly lower supersaturations. The increased hygroscopicity of oxidized soot has been attributed to the generation of polar oxygen-containing groups on the surface of particles [*Kotzick et al.*, 1997]. Formation of water-soluble organic compounds consisting primarily of humic-like aromatic polyacids (HULIS) on the particle surface has also been observed upon oxidation of soot by ozone [*Decesari et al.*, 2002].

[4] The presence of water-soluble compounds formed either from surface oxidation or condensation of semivolatile materials can also modify the structure and hygroscopic properties of soot aggregates. Soot particles emitted by diesel engines are more compact than fresh flame soot particles because the lubricating oil and semivolatile materials produced upon incomplete fuel combustion condense on soot agglomerates filling the cavities and cause restructuring [*Weingartner et al.*, 1997; *Sakurai et al.*, 2003b]. A small hygroscopic growth of the diesel and jet engine combustion soot particles (about 1.02 at 90% RH) [*Pitchford et al.*, 1991; *Hagen et al.*, 1992; *Weingartner et al.*, 1997; *Petzold et al.*, 2005] that increased somewhat upon enrichment of the fuel with sulfur [*Gysel et al.*, 2003] has been attributed to water-soluble sulfuric acid [*Grose et al.*, 2006], representing some of the condensed material. In laboratory experiments gaseous sulfuric acid has been shown to undergo irreversible uptake on soot films in a low-pressure laminar-flow reactor and also to condense on airborne fresh soot particles at atmospheric pressure, forming internally mixed aerosol [*Zhang and Zhang*, 2005]. On the basis of FTIR analysis, it has been concluded that the formation of sulfate coating is due to physical rather than chemical processes [*Zhang and Zhang*, 2005].

[5] Formation of a water-soluble coating via condensation of sulfuric acid vapor likely represents an important aging mechanism for soot in the atmosphere, affecting the particle morphology and hygroscopicity [*Zhang et al.*, 2008], the optical properties [*Fuller et al.*, 1999; *Zhang et al.*, 2008; *Khalizov et al.*, 2009], and the atmospheric lifetime [*Mikhailov et al.*, 2001]. Increased hygroscopicity and compaction can enhance the deposition of soot particles in lungs and bronchial airways, negatively affecting human health [*Boubel et al.*, 1994; *Löndahl et al.*, 2007]. The hygroscopic growth factors for ambient soot particles, such as from diesel or jet engine exhaust, measured using the tandem differential mobility analyzer (TDMA) technique have been found to be small or negligible, even though the mass fraction of water-soluble material measured independently could be as high as 15% [*Dua et al.*, 1999]. Presumably, changes in the complex morphology of soot upon humidification cause negligible particle mobility size changes with increasing RH. Using an electrodynamic balance, *Wyslouzil et al.* [1994] studied hygroscopic properties of Spherocarb carbon spheres pretreated with sulfuric acid. Although a hygroscopic mass growth of up to 1.3 at 80% RH was observed, these large (125–150 μm), spherical particles are not representative of typical submicron atmospheric soot agglomerate particles. Moreover, the mixing state of sulfuric acid in the electrodynamic balance experiments was unknown. H_2SO_4 was present either as a thin shell on the surface of spheres or was distributed within the highly porous Spherocarb material. The soluble mass fraction estimated from the growth curves was significantly lower than that from bulk analysis of particles either because of evaporation of sulfuric acid from the surface or because sulfuric acid present within the pores was inaccessible for hydration [*Wyslouzil et al.*, 1994].

[6] The knowledge of the soot particle morphology and the internal mixing state of sulfuric acid is necessary to calculate the sulfuric acid mass fraction from hygroscopic growth data and estimate the cloud activation properties. Furthermore, because of the irregular structure of soot agglomerates, determination of hygroscopicity of soot particles on the basis of particle mobility size alone is inconclusive. In this paper, we present experimental measurements of hygroscopicity for airborne soot particles with well-characterized morphology and known mass fraction of condensed sulfuric acid. Mass fractions of H_2SO_4 condensed on soot particles upon exposure to different concentrations of gas-phase sulfuric acid and the corresponding changes in the particle effective density, morphology (fractal dimension and dynamic shape factor), and optical properties are reported elsewhere [*Zhang et al.*, 2008; *Pagels et al.*, 2009; *Khalizov et al.*, 2009].

2. Experimental Section

2.1. Aerosol Generation and Sampling

[7] Soot particles were generated by incomplete combustion of propane and hexane fuels in a modified Santoro-type laminar diffusion burner [*Santoro et al.*, 1983]. The burner

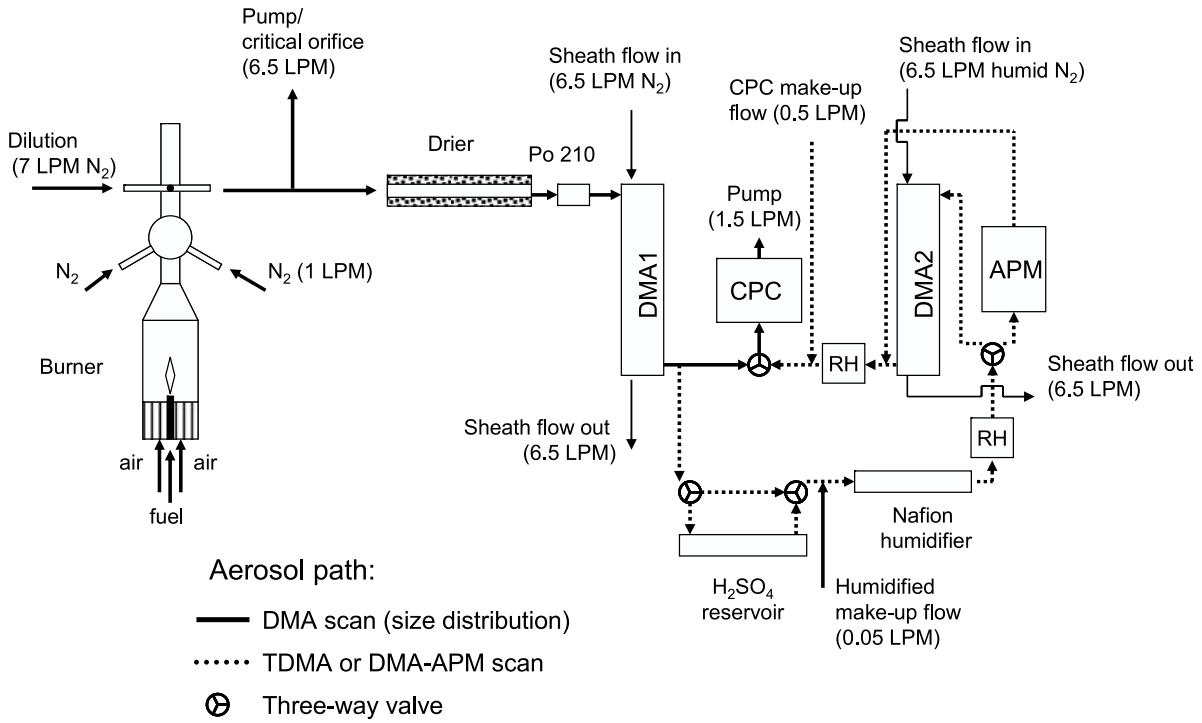

Figure 1. Schematic of the experimental setup used to generate and condition carbon soot aerosols and to measure their hygroscopic properties.

consisted of two concentric tubes, with the fuel flowing through the 7 mm i.d. inner tube and the air through the 66 mm i.d. outer tube equipped with a ceramic laminar flow element (Figure 1). Typical flow rates were 30 ml min^{-1} of propane or 100 ml min^{-1} of saturated hexane vapor in nitrogen carrier gas, and 1.7 L min^{-1} of air, resulting in a flame equivalence ratio of about 0.5 (the actual fuel-oxygen ratio divided by the fuel-oxygen ratio under stoichiometric conditions). The flame height was 5–6 cm. Approximately 7 cm above the flame tip, a 1.0 L min^{-1} nitrogen flow was introduced to mix and dilute the soot-rich flow stream with a laminar sheath flow surrounding the flame. A glass chimney was placed on the top of the burner to shield the flame from ambient disturbance and to separate the soot generation, mixing and sampling zones.

[8] The soot sampling system was similar to that described by *Kasper et al.* [1997] and consisted of a horizontally mounted stainless steel tube of 7 mm i.d. with a 0.5–1 mm orifice drilled through the wall. The tube was suspended at a height of 15 cm above the flame. The rate at which the soot-laden flow was sampled through the orifice depended on the pressure difference at the orifice, monitored with a differential pressure gauge (Magnehelic, Dwyer Instruments, Incorporated). Typically, using 7.2–6.7 L min^{-1} dilution nitrogen flow resulted in 6–10 mbar pressure drop and 0.3–0.5 L min^{-1} aerosol flow through the orifice. The dilution flow efficiently cooled the soot aerosol while keeping the relative humidity below 30%. After removing the excess flow with a pump through a critical orifice (6.5 L min^{-1}), a fraction of the diluted flow (1.0 L min^{-1}) was passed through silica gel diffusion drier and Nafion multitube drier (PD-070-18T-12SS, Perma Pure Incorporated) to further reduce the relative humidity to below 0.5%. The dry flow passed through a bipolar charger (^{210}Po, 400 μCi) to bring the aerosol particles to a predictable charge state.

[9] Polystyrene latex (PSL) spheres (nominal sizes 50 and 150 nm, Duke Scientific, Incorporated) were suspended in deionized water (17 MΩ) and atomized (3076 constant output atomizer, TSI, Incorporated). The resulting aerosol was diluted with dry nitrogen and then passed through the driers and bipolar charger as described above.

2.2. Hygroscopic Growth Measurements

[10] Measurements of soot size distributions and the particle size and mass growth were conducted using a system composed of two differential mobility analyzers (DMA 3081, TSI, Incorporated), an aerosol particle mass analyzer, and a condensation particle counter (CPC 3760A, TSI, Incorporated). The system was controlled by LabVIEW software through National Instruments DAQ interface cards. As depicted in Figure 1, the system was operated as a scanning mobility particle sizer (SMPS) [*Wang and Flagan*, 1990], a TDMA [*Rader and McMurry*, 1986; *McMurry and Stolzenburg*, 1989; *Gasparini et al.*, 2004], or a differential mobility analyzer–aerosol particle mass analyzer (DMA-APM) [*Ehara et al.*, 1996; *McMurry et al.*, 2002; *Park et al.*, 2003] by means of three-way valves.

[11] The sheath flow rate in both DMAs was maintained at 6.5 L min^{-1} using critical orifices at the outlet and volumetric flow controllers at the sheath flow inlet. Humidified N_2 was used for the sheath flow of DMA2. Two RH probes (HMM22D module with HUMICAP 180 capacitive sensor, Vaisala) were mounted before and after DMA2 to ensure a close RH value (within 2%) between the sheath flow and the sample flow. The aerosol sample flow rate through DMAs and APM was kept at 1.0 L min^{-1}. Dry nitrogen flow

was added before the CPC through a solenoid valve to make up the 1.5 L min^{-1}.

[12] In the SMPS operation mode, the instrument was used to determine the mobility particle size distribution of the aerosol. The polydisperse aerosol brought to charge equilibrium entered DMA1 and the number concentration of particles exiting DMA1 was counted by the CPC as the DMA1 voltage was continuously scanned. Particle size distributions were obtained from these data by taking into account particle charging probabilities and the instrument response, which included DMA transfer function, DMA diffusion broadening, diffusion losses in the connecting tubing, and CPC counting efficiency [*Collins et al.*, 2002].

[13] To study hygroscopicity of soot, particles of specific size were selected from the dry polydisperse aerosol flow by applying a fixed voltage to DMA1. The resulting mobility-classified aerosol was exposed to sulfuric acid vapor and then to an elevated-RH environment. The hygroscopic growth was studied as a function of RH and fresh (uncoated) particle size. In the TDMA mode, the DMA2 voltage was scanned to measure the particle size growth. A data set for a given mobility size was averaged over one up-scan and one down-scan. The diametric growth factor, *Gfd*, corresponding to the maximum count during the TDMA scan was calculated by fitting a Gaussian function to experimental data. The growth factor was expressed as a ratio of D_p/D_o, where D_p was the processed/hydrated particle diameter and D_o was the fresh particle diameter. Measurements made by bypassing the coating reservoir and humidifier were used to correct for a slight offset between DMA1 and DMA2. At least one SMPS scan was taken before each TDMA series of six to nine DMA1 particle sizes.

[14] In the DMA-APM mode, monodisperse aerosol particles were introduced into the APM to determine their mass by stepping the APM voltage at selected rotation speeds. In contrast to size classification by the DMA, which separates particles according to their electrical mobility, mass classification by the APM is independent of particle shape. The mass growth factor, *Gfm*, was expressed as a ratio of m_p/m_o, where m_p was the processed and hydrated particle mass and m_o the fresh particle mass. A detailed description of the DMA-APM methodology is provided in *McMurry et al.* [2002] and *Pagels et al.* [2009]. Relative humidities within DMA2 and APM were verified by measuring the diametric and mass growth factors of deliquesced sodium chloride and ammonium sulfate aerosol.

2.3. Soot Aerosol Coating Processes

[15] Monodisperse aerosol particles selected with DMA1 were introduced into a reservoir containing concentrated H_2SO_4 solution and then passed through a multitube Nafion humidifier (Figure 1). The acid reservoir consisted of a horizontal 50 cm long, 3 cm inner diameter Pyrex cylinder that was about half filled with an aqueous solution of sulfuric acid (86 and 96% wt H_2SO_4). The temperature of the sulfuric acid was maintained at 26 ± 1.0°C and the aerosol flow through the reservoir was equal to the sample flow rate through DMA1, 1.0 L min^{-1}. At this flow rate, the residence time of aerosol in the reservoir is estimated to be about 12 s and the sulfuric acid vapor did not achieve equilibrium with the H_2SO_4 solution [*Zhang et al.*, 1993a, 1993b].

[16] The gaseous concentration of sulfuric acid vapor was measured using ion drift – chemical ionization mass spectrometry (ID-CIMS) [*Fortner et al.*, 2004; *Zhang et al.*, 2004a]. ID-CIMS measurements were performed offline using identical flow and temperature conditions as in soot aerosol experiments. Neutral sulfuric acid molecules were converted to ions through the ion-molecule reaction using $(NO_3^-)(HNO_3)_n$ reagent ions in the ion drift tube,

$$H_2SO_4 + \left(NO_3^-\right)(HNO_3)_n \rightarrow HSO_4^-(HNO_3)_n + HNO_3, k_n \quad (1)$$

where k_n is the ion-molecule reaction rate constant, $n = 0..2$ [*Viggiano et al.*, 1997]. The concentration of sulfuric acid, $[H_2SO_4]$, was then determined by

$$[H_2SO_4] = S\left(HSO_4^-(HNO_3)_n\right)/\{S\left(\left(NO_3^-\right)(HNO_3)_n\right) \times k_n \times dt\}, \quad (2)$$

where $S((NO_3^-)(HNO_3)_n)$ and $S(HSO_4^-(HNO_3)_n)$ are the measured signals of the reagent and product ions, respectively, and $dt = l/U$ determined from the length of the drift tube (l) and the reagent ion drift velocity (U). The vapor concentrations of sulfuric acid in the gas flow passing above the 96 wt % and 86 wt % H_2SO_4 aqueous solutions were estimated to be 1.4×10^{10} (high) and 2.5×10^9 (low) molecules cm^{-3}, respectively. This was approximately twenty-fold below the saturation vapor pressure of sulfuric acid above corresponding solutions [*Perry and Green*, 1997]. To avoid significant depletion of the gas-phase H_2SO_4 due to condensation on particles, all coating experiments were performed using low enough number concentration of mobility-classified aerosol. The maximum allowable values were estimated from the absolute mass of sulfuric acid condensed per particle and the concentration of gaseous sulfuric acid in the coating reservoir, e.g., for 100 nm soot aggregates aerosol number density was kept below 2000 cm^{-3}.

[17] At the high H_2SO_4 concentration, the formation of new particles with number concentration up to 300 cm^{-3} was occasionally observed. These particles were formed by homogeneous binary nucleation of sulfuric acid with the residual water vapor penetrating through DMA1 (RH < 0.1%) [*Zhang et al.*, 2004a]. Because of their significantly smaller size (less than 10 nm) and low concentration, these nucleated particles had negligible contribution to the coating and were effectively separated from soot and PSL in DMA2 and APM.

[18] The gaseous concentration of H_2SO_4 over coated soot particles increased strongly as the relative humidity was reduced below 5% and the coated sulfuric acid became highly concentrated. The RH at the outlet of DMA1 located upstream of the reservoir was below 0.1%. Therefore, there was a concern that sulfuric acid, once condensed onto the aerosol particles, could evaporate during transport to the humidifier or during the dry diameter measurements, within DMA2 and the APM. To suppress evaporation of sulfuric acid from the coated soot particles, immediately following the H_2SO_4 exposure the RH was adjusted to 5% to stabilize H_2SO_4. This was accomplished by adding 50 ml min^{-1} of humidified nitrogen (after passing through a water bubbler and a filter) a few centimeters downstream the H_2SO_4

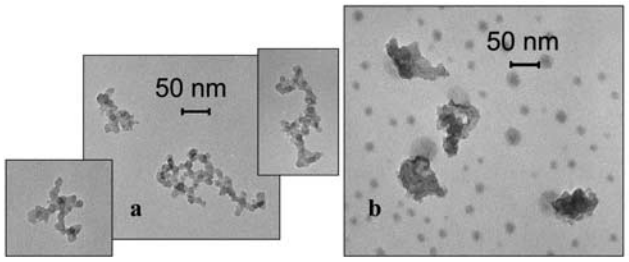

Figure 2. Transmission electron microscopy images of (a) fresh soot agglomerates and (b) soot exposed to 1.5×10^{10} cm^{-3} H_2SO_4 vapor for 12 s.

reservoir. We observed that the addition of the humidified flow did not produce new particles and effectively suppressed the evaporation of sulfuric acid.

[19] Following the exposure to sulfuric acid and stabilization at 5% RH, the relative humidity was further adjusted in the range 5% to 90% using a multitube Nafion humidifier (PD-070-18T-24SS, Perma Pure, Incorporated). The humidification procedure was based on the design of *Gasparini et al.* [2004].

2.4. TEM Analysis

[20] The morphology of soot particles was examined using a JEOL 2010 transmission electron microscope (TEM), which was operated at an accelerating voltage of 100 kV. Samples of the soot-containing aerosols were collected downstream of DMA1 and the processing chamber on Cu TEM grids (200 mesh with amorphous carbon film) using a low-pressure impactor [*Hering et al.*, 1979]. TEM images of the aerosol samples were obtained at magnifications ranging from 5,000 to 50,000.

3. Results and Discussion

3.1. Soot Morphology

[21] The fresh soot from a propane flame with an equivalence ratio of 0.5 (the actual fuel to oxygen ratio divided by the fuel to oxygen ratio under stoichiometric conditions) displays chain-like aggregate structures with the spherical primary particles clearly identifiable (Figure 2a). For a flame with a higher equivalence ratio of 1.25, the primary particles appear more blended, with less clear boundaries. The morphology and chemical composition of soot closely relate to the global equivalence ratio of the flame [*Widmann et al.*, 2003]. Under the stoichiometric conditions, the spherical primary particles are clearly noticeable, but when the equivalence ratio is increased, they may appear to be fused because of condensed organic material produced in a fuel-rich flame. In our experiments, to avoid condensation of organics, soot is always generated under relatively air-rich conditions with the equivalence ratio of about 0.5. The average primary particle diameter measured under these conditions is 15 ± 1 nm.

[22] A typical size distribution of fresh soot aerosol produced by burning propane in a diffusion flame with equivalency ratio of 0.5 is shown in Figure 3. As reported previously [*Maricq et al.*, 2003], the mean agglomerate mobility size increases with both the enhanced equivalence ratio and elevated flame height. The fuel and airflow rates and the fuel/air ratios chosen in our study result in a size distribution with a geometric mean diameter of about 130 nm and geometric standard deviation of 1.8. For typical dilution flow values used in our experiments, the dilution ratio of the sample was found to have little effect on the morphology of fresh soot agglomerates. Under these conditions, the concentration of organic material in the particle phase is minimal, while the size distribution of soot is broad enough to select fresh soot particles with mobility sizes in the range from 30 to 400 nm for TDMA and DMA-APM measurements.

[23] Exposure of soot aerosol to sulfuric acid vapor significantly changes the appearance of soot samples (Figure 2b). Soot agglomerates become more compact. The condensed sulfuric acid is observable as a residue on the particles and separate droplets are also observed. The droplets are not spread uniformly throughout the TEM grid, but rather cluster around the soot particles suggesting that they are produced by splattering the sulfuric acid coating from soot agglomerates upon high-velocity impaction on the TEM grid in the low-pressure impactor. Sulfuric acid on the TEM grid is stable enough under vacuum conditions in the TEM chamber. However, at the highest magnifications, the droplets are prone to evaporation due to exposure to the heat produced by the electron beam, confirming their volatile nature.

3.2. Hygroscopic Growth

[24] Unlike most previous studies, we investigate the hygroscopic properties of airborne soot particles with well-characterized morphology and mixing state. The mass fraction of H_2SO_4 coating is size-dependent, decreasing monotonically with initial particle mobility size [*Zhang et al.*, 2008; *Pagels et al.*, 2009]. The mass fractions of anhydrous H_2SO_4 calculated from DMA-APM growth factors using water activity data for the H_2SO_4-H_2O system [*Perry and Green*, 1997] are found to vary in the range 0.18–0.09 and 0.43–0.35 for 50–360 nm soot particles exposed to the low and high H_2SO_4 vapor concentrations, respectively.

[25] As mentioned above, to suppress sulfuric acid evaporation of the coated soot particles, the RH of aerosols

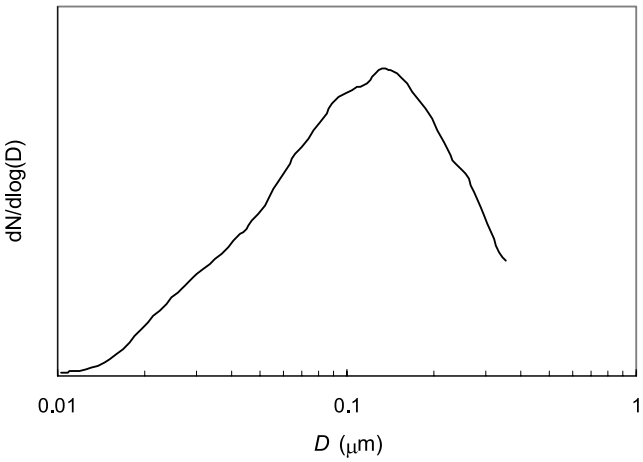

Figure 3. Number size distribution of fresh (unprocessed) carbon soot aerosol produced in a modified Santoro-type burner operating on propane/air diffusion flame with equivalency ratio of 0.5.

following H_2SO_4 exposure is adjusted to 5%. To investigate whether residual evaporation could potentially affect our data, a series of measurements of the mobility growth factor of H_2SO_4-coated (1.4×10^{10} molecules cm^{-3}) 50 nm PSL spheres are conducted using the TDMA for RH < 1% and RH 5% (corresponding to experiments with and without the saturated makeup flow). The residence time from the coating reservoir to DMA2 is varied from 5 s (typically used throughout the study) to 30 s and 90 s. The detected growth factors for the 5, 30 and 90 s residence times are 1.14, 1.06, 1.03 at RH < 1% and 1.23, 1.22, 1.24 at RH 5%, indicating that H_2SO_4 is lost from particles by evaporation after leaving the H_2SO_4 reservoir only at dry conditions. Thus, the effect of sulfuric acid evaporation is negligible for the data reported in this paper.

3.2.1. DMA-APM

[26] The effect of relative humidity on the mass growth of soot is investigated for particles of initial diameters ranging from 50 to 240 nm at relative humidities of 5, 50, and 80%. Humidification of fresh (uncoated) soot aerosol has little effect on the particle mass. At 80% RH, measured mass growth factors are 1.01 and 1.08 for 50 and 240 nm particles, respectively, indicating very small fraction of water soluble compounds on the surface of soot agglomerates. When coated soot (H_2SO_4 concentration 1.4×10^{10} molecules cm^{-3}) is exposed to elevated RH, the particle mass increases because of condensation of water and formation of an aqueous-sulfuric acid shell (DMA-APM results in Figure 4). Soot particles with smaller initial size display higher hygroscopic growth, indicating that they contain more soluble material. The mass growth factors measured at different relative humidities were used to calculate the mass fractions of sulfuric acid coating of the coated particle mass (f_m) according to equations 3 and 4:

$$f_m = \left[\left(\frac{1}{f_{m,RH}} - 1\right) \times \frac{100}{x_{RH}} + 1\right]^{-1} \quad (3)$$

$$f_{m,RH} = 1 - m_0/m_p, \quad (4)$$

where m_o and m_p is the mass of fresh and coated soot particles, x_{RH} is the equilibrium weight percent concentration of sulfuric acid solution at relative humidity RH (Kelvin effect included), $f_{m,RH}$ is the mass fraction of x_{RH} sulfuric acid aqueous solution of the coated particle mass. Table 1 shows that f_m averaged over the measurements performed at three different relative humidities agree with each other within 10%. The mass fractions of sulfuric acid are further used in combination with effective densities of fresh soot to calculate absolute masses of sulfuric acid and soot in the coated agglomerates (DMA-APM results in Table 1).

3.2.2. TDMA

[27] The hygroscopic growth of fresh and H_2SO_4-coated soot is investigated for particles with initial diameters from 30 to 360 nm and RH between 5 and 90%. Figure 5a shows an example of the TDMA scan for fresh propane soot at 5% RH. The TDMA curves for particles of different sizes practically overlap and no change is observed upon increase of relative humidity up to 90%. The growth factors for particles of all sizes calculated from Gauss fits are 1.00 ± 0.02

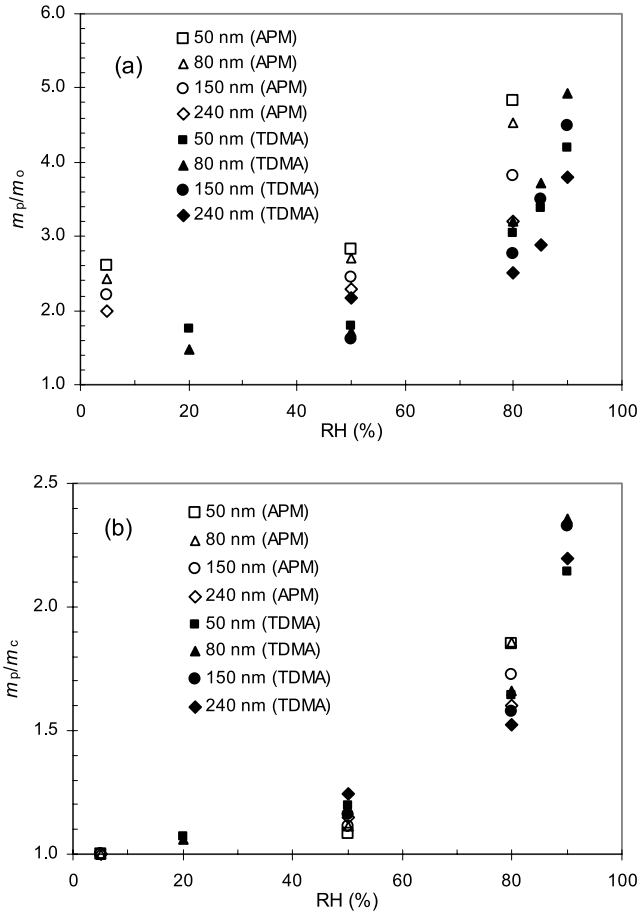

Figure 4. Hygroscopic mass growth factor of H_2SO_4-coated propane soot agglomerates with mass m_p as a function of relative humidity: (a) relative to fresh agglomerates, $Gfm_o = m_p/m_o$ (m_o is the mass of fresh soot particles), (b) relative to coated agglomerates, $Gfm_c = m_p/m_c$ (m_c is the mass of coated soot particles at 5% relative humidity (RH)). Soot particles were exposed to high concentration of sulfuric acid vapor (1.4×10^{10} molecules cm^{-3}). Open symbols represent the mass growth factors measured experimentally by differential mobility analyzer-aerosol particle mass analyzer (DMA-APM) at 5, 50, and 80% RH. Solid symbols represent the mass growth factors calculated from tandem differential mobility analyzer (TDMA) diametric growth data measured at 20, 50, 80, and 90% RH assuming complete restructuring of the cores.

in the RH range of 5 to 90%, indicating no particle growth or shrinking within the detection sensitivity of our TDMA. This is in contrast to previous studies, which reported that diesel and aircraft engine soot from "sulfur-free" fuels could take up water under subsaturated conditions and act as contrail nuclei [*Weingartner et al.*, 1997]. It is likely that soot emitted from combustion engines contained water-soluble organic carbon and sulfuric acid [*Gysel et al.*, 2003] and is therefore slightly hygroscopic whereas the flame soot generated under well-ventilated conditions in the present study contains no volatile materials. Also, carbon particles produced by spark discharge in the inert gas atmosphere were found to shrink to about 85% of the dry size at 90% RH [*Weingartner et al.*, 1995]. This shrinkage is

Table 1. Mass Fraction of Sulfuric Acid and the Absolute Soluble and Insoluble Particle Mass[a]

	Soluble Mass Fraction		Mass soluble (fg)		Mass Insoluble (fg)	
D_o (nm)	TDMA[b]	APM[b]	TDMA	APM	TDMA	APM
			High Sulfuric Acid Concentration			
50	0.38 ± 0.01	0.50 ± 0.05	0.04	0.04	0.06	0.04
$50^{(PSL)}$	0.49	0.44	0.08	0.05	0.08	0.07
79	0.43 ± 0.03	0.47 ± 0.04	0.12	0.10	0.16	0.12
155	0.39 ± 0.04	0.43 ± 0.04	0.45	0.36	0.70	0.47
$155^{(PSL)}$	0.16	0.15	0.40	0.33	2.18	1.94
240	0.34 ± 0.03	0.39 ± 0.02	1.00	0.79	1.95	1.25
360	0.33 ± 0.02	0.41	2.09	1.69	4.29	2.47
			Low Sulfuric Acid Concentration			
50	0.108	0.198	0.008	0.009	0.07	0.04
79	0.068	0.162	0.016	0.022	0.21	0.12
155	0.036	0.145	0.047	0.080	1.25	0.47
240	0.021	0.133	0.091	0.191	4.34	1.25
360	0.001	0.096	0.019	0.304	14.60	2.88

[a]Calculated from tandem differential mobility analyzer (TDMA) diametric and differential mobility analyzer-aerosol particle mass analyzer (DMA-APM) mass growth factors for soot aggregates and Polystyrene latex (PSL) spheres of different initial diameters after exposure to 1.4×10^{10} (high) and 2.5×10^{9} molecules cm^{-3} (low) gaseous H_2SO_4. Hygroscopic growth factors of soot measured by TDMA are corrected using the diameters of restructured agglomerates at 5% relative humidity (RH) (coated, humidified to 90% RH, and redried to 5% RH) [*Pagels et al.*, 2009].

[b]For soot particles exposed to high concentration of sulfuric acid vapor, the errors represent standard deviations for data averaged over the measurements performed at several relative humidities (80, 85, and 90% RH for TDMA measurements and 5, 50, and 80% RH for DMA-APM measurements).

attributed to the collapse of highly branched particles following the capillary condensation of water in small angle cavities of the aggregates. Although the flame soot in our study is also highly aggregated (Figure 2a), no apparent restructuring is observed. It is plausible that the spark-generated soot exhibits different surface chemical compositions and structures than the flame soot that increases its tendency to absorb water and undergo subsequent restructuring.

[28] Considerable changes in the TDMA distributions are observed for soot particles exposed to sulfuric acid vapor concentration of 1.4×10^{10} molecules cm^{-3} (Figure 5b). The effect of initial size on the hygroscopic behavior of coated soot particles is clearly evident, especially at high relative humidities. At 80% RH (Figure 5c), particles with mobility diameter smaller than 80 nm experience growth whereas particles larger than 155 nm exhibit a decrease in mobility size. Soot particles with initial sizes in the range 80–245 nm display slightly bimodal TDMA distributions caused by the presence of doubly and triply charged particles in the monodisperse aerosol sample produced by DMA1. Multiply charged particles have the same electrical mobility as singly charged particles yet significantly larger size. The contribution of multiply charged particles at each size depends on the shape of the polydisperse soot size distribution and particle charging probability. The concentration of multiply charged particles in monodisperse aerosol is minimal for 30–50 nm particles because they have the lowest probability of carrying multiple charges and also for 360 nm particles because they are sampled at the descending shoulder of the size distribution where the concentration of larger particles is negligible (Figure 3). As a result, the effect of multiply charged particles is minimal for the smallest and largest soot aggregates. Using a second Po-210 diffusion charger in front of DMA2, we directly quantified the fraction of doubly and triply charged particles in the mobility-classified fresh soot aerosol. For the size distribution shown in Figure 3, this fraction was the highest when the DMA1 voltage was set to transmit 100 nm particles, in good agreement with the trend shown in Figure 5c.

[29] We used the TDMA data to calculate diametric growth factors, D_p/D_o, where D_p is coated and D_o is uncoated (fresh) soot particle diameters at different RH. In cases where two modes are evident in the TDMA distributions, bimodal

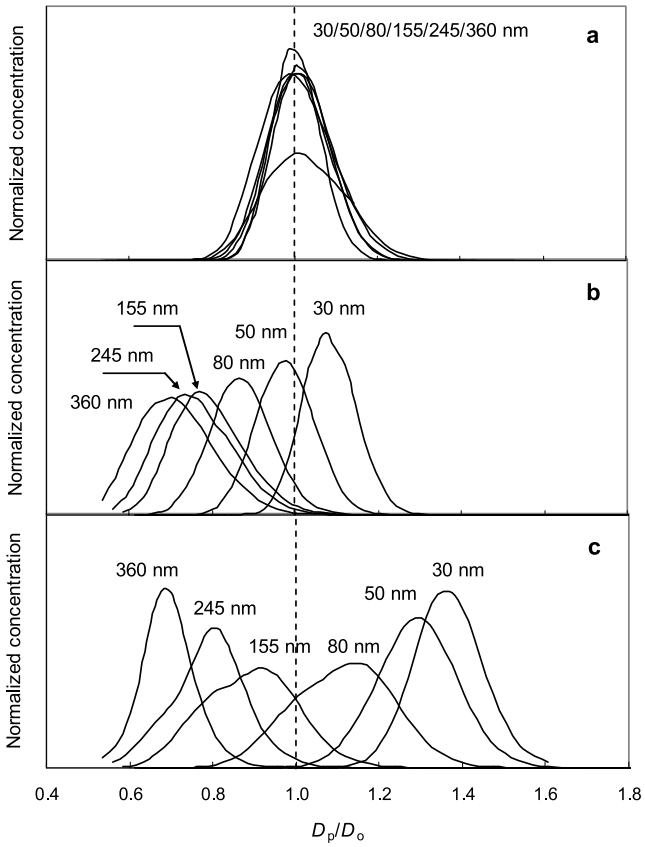

Figure 5. TDMA data for fresh (a) and coated (b and c) propane soot aerosols for various fresh soot sizes: (a) and (b) 5% RH; (c) 80% RH. D_p/D_o is the hygroscopic growth factor. Soot aerosol was coated using the high-concentration H_2SO_4 (1.4×10^{10} cm^{-3}).

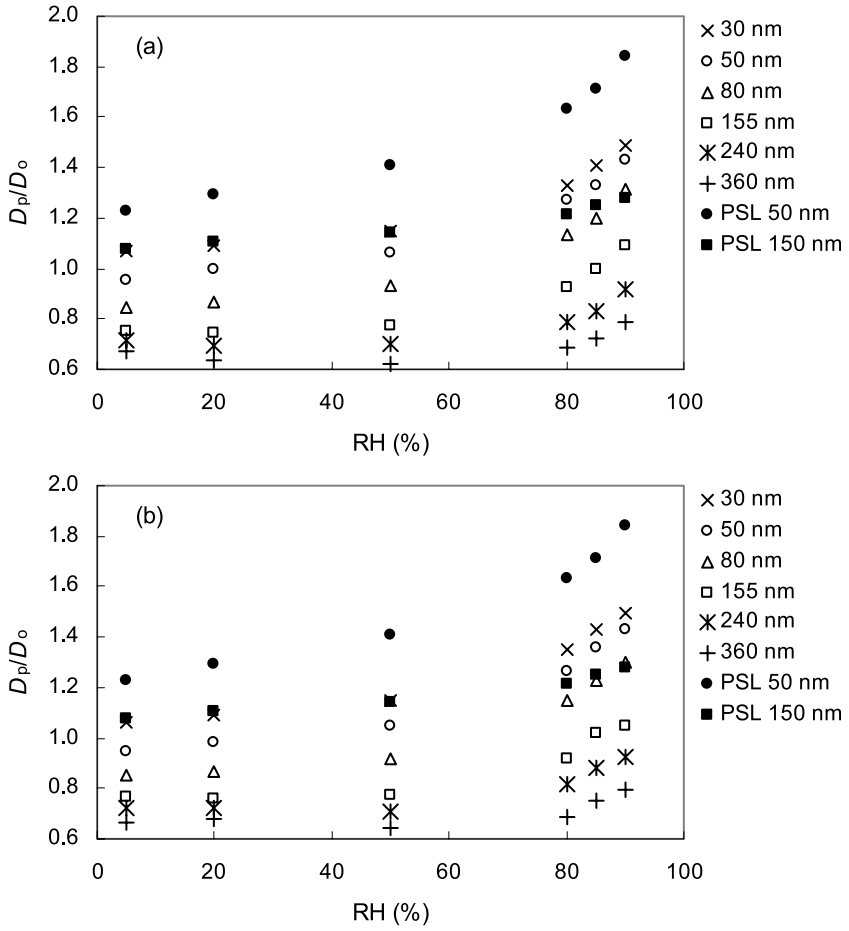

Figure 6. Hygroscopic growth, D_p/D_o, of (a) propane and (b) hexane soot exposed to 1.4×10^{10} cm^{-3} sulfuric acid vapor as a function of fresh soot particle mobility size and RH (D_p denotes processed particle diameter, D_o - fresh particle diameter). For comparison, the growth curves for 50 and 150 nm Polystyrene latex (PSL) spheres processed under identical conditions are also shown.

fits are employed. The mode with the larger growth factor corresponds to singly charged particles because they are denser than doubly charged particles of the same electrical mobility and hence exhibit less restructuring and larger hygroscopic growth. Figure 6 displays the dependences of the growth factor on relative humidity (hygroscopic growth curves) for soot particles and PSL spheres of different initial sizes exposed to sulfuric acid vapor concentration of 1.4×10^{10} molecules cm^{-3}. Coated soot particles from propane (Figure 6a) and hexane (Figure 6b) flames show identical hygroscopic growth behavior, suggesting that soot produced from different hydrocarbon fuels in lean flames has similar morphology and chemical composition. However, significant differences are observed between the growth curves of coated soot aggregates and coated PSL spheres. Coated PSL spheres display noticeable growth even at RH 5%, and the growth factors increase with relative humidity and reach the values of 1.84 and 1.28 at RH 90% for the initial mobility diameters of 50 and 150 nm, respectively. The absolute thickness of the aqueous H_2SO_4 layer on PSL spheres calculated using hygroscopic growth factors is practically independent of the initial particle size and only varies with relative humidity, increasing from 5.7 to 21.1 nm in the 5–90% RH range.

[30] Coated soot aggregates, on the contrary, exhibit a decrease in size at RH 5%, with the exception of the smallest 30 nm particles, which show minor restructuring because of a higher initial density. An increase in relative humidity leads to two different patterns in the hygroscopic growth of coated soot. Particles with $D_o \leq 80$ nm grow, reaching a growth factor of 1.49–1.32 (30–80 nm) at RH 90%. Particles with $D_o \geq 155$ nm shrink at the intermediate RH, but start to grow at higher relative humidities. The growth curves have a pronounced minimum between 20 and 50% RH, and the location of the minimum depends on the particle initial diameter. At this RH, particles approach spherical shapes and their volume equivalent and mobility diameters become identical. At RH 90%, the growth factors of 155–360 nm soot particles are in the range 1.09–0.79. It is evident from Figure 6 that for the largest agglomerates the restructuring upon condensation of water dominates over the growth of the aqueous shell even at the highest RH, with a net effect of decreasing particle mobility size.

[31] The hygroscopic growth factors presented in Figure 6 are measured relative to fresh (uncoated) soot particle diameters because in our experiments fresh soot particles are mobility-classified first and then coated. Most laboratory

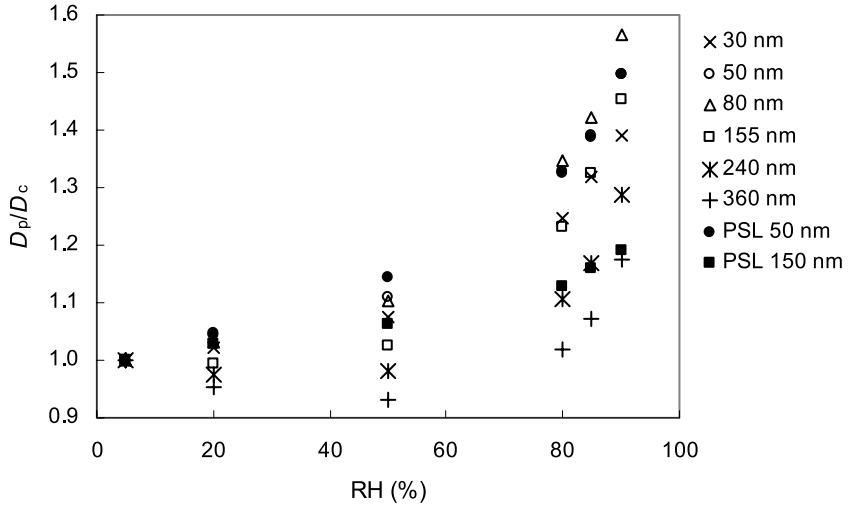

Figure 7. The data for propane soot from Figure 5 transformed into a form of D_p/D_c typically used to report laboratory and field hygroscopic growth measurements (D_p denotes particle diameter at RH $\geq$ 5%, D_c is H_2SO_4-coated particle diameter at 5% RH). The legend shows fresh (uncoated) particle diameters. The growth factors for 50 nm soot and PSL particles practically overlap.

and field studies report the growth factors in reference to the diameter of coated particles at dry conditions, typically at RH < 15%. The growth factors measured relatively to fresh soot (Figure 6) can be transformed to this commonly used form with equation 5,

$$Gfd_c = D_p/D_c = (D_p/D_o)/(D_c/D_o), \quad (5)$$

where D_c is the mobility diameter of coated particles at 5% RH (D_c = 32, 48, 68, 116, 170, and 240 nm for soot particles with initial uncoated mobility diameters D_o = 30, 50, 80, 155, 240, and 360 nm, respectively). By definition, $D_p/D_c = 1$ at RH 5%, which is selected as the reference state. At RH < 5% sulfuric acid evaporates quickly from particles and the weight percent sulfuric acid in aqueous solutions is strongly dependent on RH.

[32] As shown in Figure 7, the transformation according to equation 5 results in a substantial change in the appearance of the hygroscopic growth curves. The highest growth factor at 90% RH is now observed for 80 nm soot, which is followed in the decreasing order by 50 nm soot and 50 nm PSL (overlap), and then 155 nm, 30 nm and 240 nm soot particles. The lowest growth factor at 90% RH is observed for 150 nm PSL and 360 nm soot particles. The patterns presented in Figure 7 indicate that hygroscopic growth is determined by three major factors: the fraction of sulfuric acid coating, the degree of restructuring of the insoluble core at 5% versus higher RH, and the increase in saturation vapor pressure above the particle surface due to the Kelvin effect. Growth curves for coated soot aggregates and PSL spheres with initial diameters of 50 nm practically overlap because particles of both types acquire similar mass fractions of sulfuric acid coating (Table 1). Since 50 nm soot aggregates restructure almost completely at RH 5%, their hygroscopic behavior is well described using the insoluble core model assuming a spherical core. Smaller growth of 30 nm soot particles and larger growth of 80 nm soot particles relative to that of 50 nm particles is in part due to the Kelvin effect, which acts to reduce (30 nm) or increase (80 nm) the amount of condensed water. The smaller fraction of condensed sulfuric acid mass and gradual restructuring of soot cores at increasing RH both contribute to progressively smaller growth of coated soot agglomerates with initial diameters of 152 nm and larger.

[33] Exposure of soot aggregates to a lower sulfuric acid concentration (2.5×10^9 molecules cm^{-3}) results in less H_2SO_4 coating. Figure 8 shows that the mobility growth factor D_p/D_o expressed relative to fresh (uncoated) soot diameter shifts with increasing relative humidity for these particles. At RH 5%, particles of all sizes experience only a minor shrinking with an average $Gfd = 0.98 \pm 0.01$. Increasing relative humidity to 50% causes a marginal variation in mobility growth factors, and only at RH $\geq$ 80% distinct changes in Gfd are observed. The smallest particles (30 nm) display a maximum growth of less than 1.2 at 90% RH whereas coated soot agglomerates larger than 155 nm continue to shrink even at 90% RH. It should be noted that the transformation of these growth curves according to equation 5 had little effect because for this low sulfuric acid concentration, D_c differed from D_o by less than 2%.

3.2.3. Interpretation of TDMA Data

[34] Hygroscopic mobility growth factors measured by TDMA are commonly used to derive the soluble volume fraction of coated particles by assuming that the particle mobility diameter is identical to the volume equivalent diameter. In the case of coated soot, however, the mobility diameter is significantly larger than the volume equivalent diameter and approaches the latter only when coated agglomerates are transformed into a compact form at sufficiently high relative humidity. In our experiments, this condition is fulfilled for soot particles with initial mobility diameters of 30–80 nm exposed to sulfuric acid concentration of 1.4×10^{10} molecules cm^{-3}. These small particles restructure almost completely at 5% RH and TDMA measurements over the entire 5–90% RH range can be used to

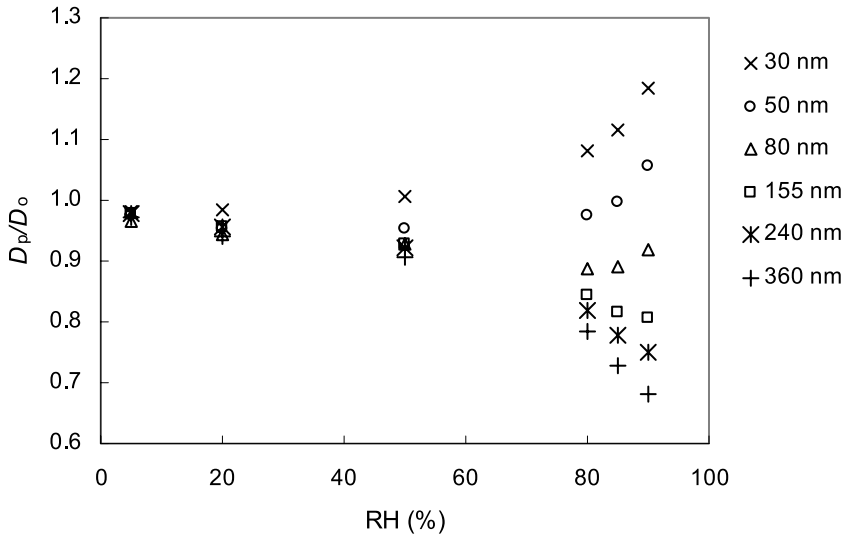

Figure 8. Hygroscopic growth, D_p/D_o, of propane soot exposed to 2.5×10^9 cm^{-3} sulfuric acid vapor as a function of fresh soot particle mobility size and RH (D_p is processed particle diameter, D_o is fresh particle diameter).

calculate particle soluble fractions. For larger particles, however, accurate data can be derived only from high RH measurements (Figure 7). The effect of changing morphology upon humidification is most notable for soot exposed to sulfuric acid concentration 2.5×10^9 molecules cm^{-3}. Even at high relative humidity the restructuring of soot cores is incomplete (Figure 8) and no meaningful information can be inferred from such TDMA data. Similar observation has been made by *Dua et al.* [1999] who, using TDMA, detected no appreciable growth for soot particles produced by a diesel engine, even at RH > 99%. At the same time, the soluble fraction of these particles, measured by collection on filters and extraction, was found to be about 15%.

[35] One approach to eliminate the bias in hygroscopic growth data caused by soot compaction during internal mixing is to preprocess the aerosol by exposing the coated soot aggregates to a high RH cycle prior to TDMA measurements [*Swietlicki et al.*, 2008]. Increasing RH of aerosol up to 90–99% forces the agglomerates to restructure. Subsequent drying of aerosol to 5% RH removes condensed water and brings soot particles to an appropriate reference state. In this way, hygroscopic growth factors are measured relative to fully compacted coated particles. However, the volume growth is still underestimated since water condensing on the particles initially fills the remaining voids.

[36] An alternative way to correct the existing "imperfect" TDMA measurements, such as those shown in Figures 6 and 8, is by recalculating hygroscopic growth factors using diameters of coated soot particles subjected to a high-humidity cycle (D_{cycled}) as reference "dry" diameters (equation 6).

$$Gfd_{cycled} = D_p/D_{cycled} = (D_p/D_o)/(D_{cycled}/D_o) \quad (6)$$

[37] Figure 9 shows that this transformation cancels the contribution of restructuring to the growth of soot particles exposed to 1.4×10^{10} molecules cm^{-3} concentration H_2SO_4 for relative humidities above 50%. However, for soot exposed to 2.5×10^9 molecules cm^{-3} H_2SO_4, only the growth factors measured at 90% RH are properly corrected. In both cases, the corrected TDMA hygroscopic growth factors have weaker size dependence than uncorrected data, in good agreement with DMA-APM measurements that show moderate reduction in the mass fraction of sulfuric acid coating with increasing initial particle size.

[38] The corrected TDMA growth factors measured at 80–90% RH (1.4×10^{10} molecules cm^{-3} H_2SO_4) and 90% RH (2.5×10^9 molecules cm^{-3} H_2SO_4) are used with insoluble core Köhler theory [*Seinfeld and Pandis*, 1998; *Gasparini et al.*, 2004] to calculate absolute masses and volume fractions of sulfuric acid on soot particles, taking into account the Kelvin effect. Also, assuming the complete restructuring of soot cores and using an inherent material soot density of 1.78 g cm^{-3} [*Park et al.*, 2004], the insoluble core mass and the mass fraction of sulfuric acid are estimated. Table 1 reveals that the TDMA method overestimates the soluble and insoluble particle masses and the deviation between the data inferred from TDMA and DMA-APM measurements increases with initial particle size. For soot particles exposed to higher H_2SO_4 concentration, errors in the absolute soluble and insoluble masses cancel out and soluble mass fractions calculated from TDMA and DMA-APM measurements agree reasonably. However, in the case of soot particles exposed to the lower-H_2SO_4 concentration, TDMA fails to reproduce the results of DMA-APM measurements, even after correction.

[39] After exposure to H_2SO_4, soot agglomerates restructure to a more compact form but their shape is still nonspherical (Figure 2b). When the particle soluble fraction is small, even at high RH the solution shell is unable to envelope the soot core completely and the coated core approximation becomes invalid. This is illustrated in Figure 4a, where even for soot with high coating fraction, mass growth factors (m_p/m_o) calculated from TDMA hygroscopic data relative to the fresh soot particle mass (Table 1) are still

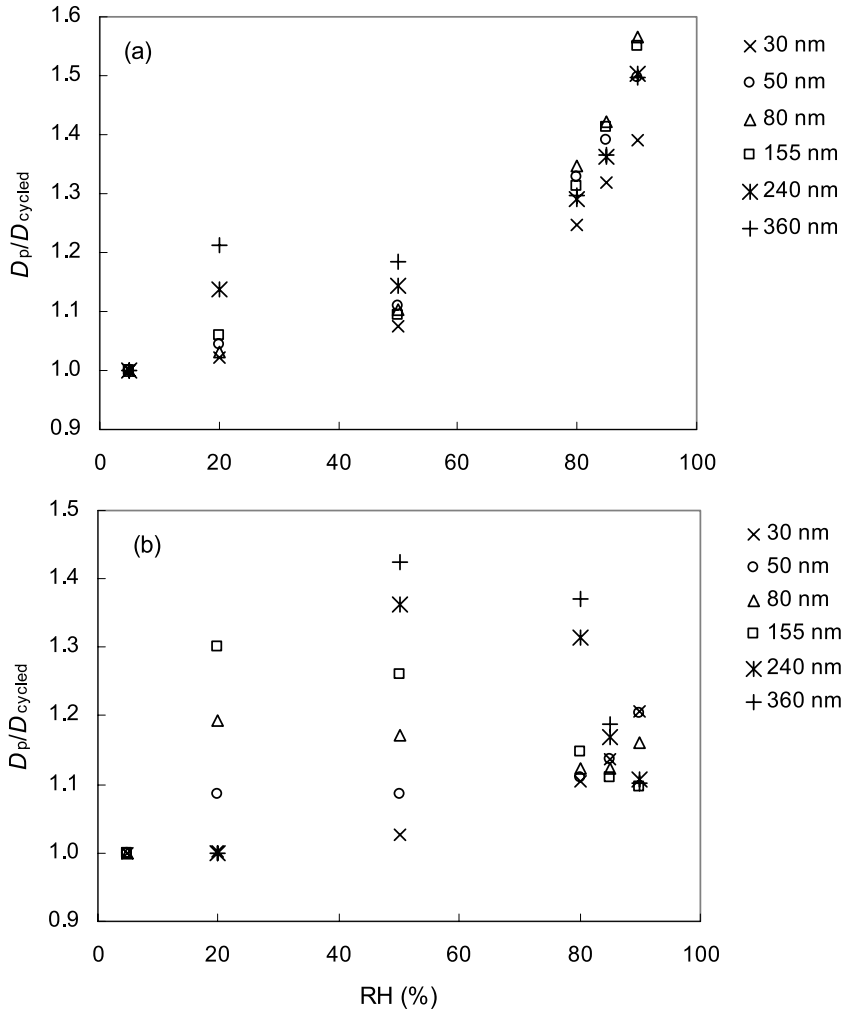

Figure 9. Mobility growth factors calculated using restructured reference diameter, D_{cycled}, for soot particles exposed to (a) high (1.4×10^{10} cm^{-3}) and (b) low (2.5×10^{9} cm^{-3}) concentration sulfuric acid vapor (D_p denotes particle diameter at RH $\geq$ 5%, D_{cycled} - diameter of H_2SO_4-coated particles subjected to high RH cycle). The legend shows fresh (uncoated) particle diameters.

lower than the growth factors measured directly by DMA-APM. However, when coated soot aggregates at 5% RH are used as a reference state to calculate the m_p/m_c mass growth factors typically reported in most other studies, the effects caused by nonspherical shape and changing morphology are partially canceled, leading to a better apparent agreement between the mass growth factors inferred from TDMA data and those measured directly by DMA-APM (Figure 4b).

[40] Soot particles of a given mobility size have a much smaller mass than PSL particles of the same size because of the agglomerated structure. Since both soot and PSL particles take up similar amount of H_2SO_4, the net result is that the mass fraction of sulfuric acid on the agglomerates is higher than on PSL (Table 1). Upon exposure to sulfuric acid and water, the density of the soot core increases, resulting in weaker dependence of condensed mass fractions and diametric hygroscopic growth factors on initial particle size. Similar weak size dependence have also been observed in our earlier TDMA study [*Zhang et al.*, 2008], where because of somewhat different experimental setup, coated and partially restructured soot agglomerates were size-selected by DMA1 for hygroscopic measurements.

[41] In a recent study of jet engine combustion particles, the hygroscopic growth factors were found to increase distinctively with decreasing dry particle size, suggesting a higher H_2SO_4 volume fraction in smaller particles [*Gysel et al.*, 2003]. The authors attribute the size dependence of H_2SO_4 fraction to the relatively larger mass accommodation of smaller particles leading to more condensation of gaseous sulfuric acid. However, the mass accommodation coefficients of sulfuric acid on a variety of particle types all approach a value of unity [*Jefferson et al.*, 1997]. Although restructuring of soot particles is taken into account by *Gysel et al.* [2003] through the use of a mobility correction factor, this factor is assumed to be RH independent. Our measurements indicate that for soot coated with small H_2SO_4 volume fractions, the correction factor will change with relative humidity. Thus, the observed strong dependence of H_2SO_4 mass accommodation on particle size likely represents an artifact of the TDMA

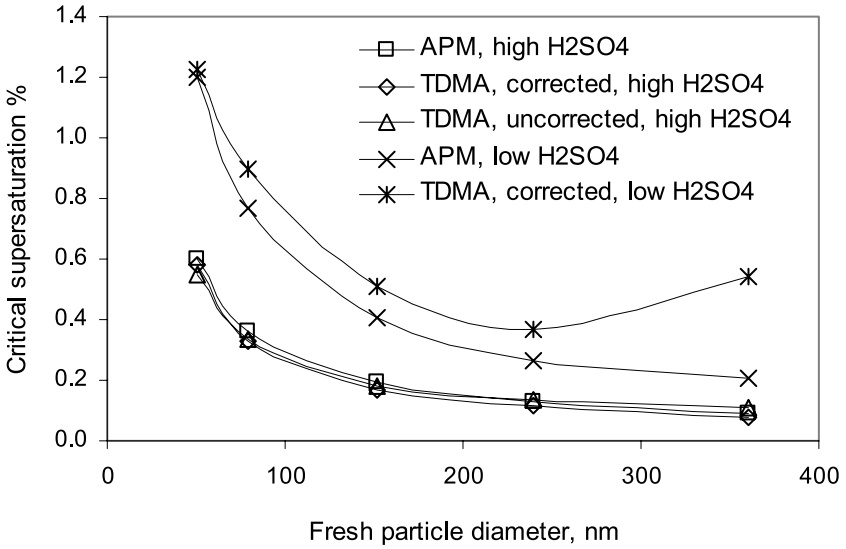

Figure 10. Critical supersaturations for activation of H_2SO_4-coated propane soot particles to cloud droplets calculated using sulfuric acid coating fractions from TDMA (at 90% RH) and DMA-APM (5–80% RH) measurements. Soot particles were exposed to high (1.4×10^{10} molecules cm^{-3}) and low (2.5×10^{9} molecules cm^{-3}) concentrations of sulfuric acid.

measurements caused by restructuring of soot agglomerates with increasing RH. It is also possible that soot particles from the jet engine are initially more compact than the particles in our study because of condensation of nonhygroscopic organic material. As shown above, the mass fraction of condensed sulfuric acid shows stronger dependence on the particle diameter for compact particles. The uncertainty about the relation between morphology and hygroscopic properties of the jet engine soot can be clarified by measuring the particle effective density and fractal dimension.

3.3. Atmospheric Implications

3.3.1. CCN Activation of H_2SO_4 Coated Soot

[42] Hygroscopic properties measured under subsaturated conditions can be used to evaluate the ability of coated soot particles to serve as cloud condensation nuclei (CCN). Aerosol particles activate to cloud droplets at ambient supersaturations that are higher than the critical supersaturation, S_{crit}, which is defined as the peak supersaturation on the Köhler curve. We use the results from our DMA-APM and TDMA hygroscopic growth measurements (Table 1) with insoluble core Köhler theory [*Gasparini et al.*, 2004; *Seinfeld and Pandis*, 1998] to calculate critical supersaturations, assuming that the soot cores restructure completely at 90% RH and the inherent material soot density is 1.78 g cm^{-3} [*Park et al.*, 2004]. As illustrated in Figure 10, a close agreement is observed between S_{crit} calculated from DMA-APM and TDMA hygroscopic data for soot aggregates exposed to sulfuric acid vapor with concentration of 1.4×10^{10} molecules cm^{-3}. The use of either corrected or uncorrected TDMA data produces similar S_{crit}. However, for soot exposed to 2.5×10^{9} molecules cm^{-3} H_2SO_4, critical supersaturations calculated from TDMA data are always higher than the DMA-APM based values and the deviation increases with initial particle size.

[43] Critical supersaturations of soot exposed to low concentration of sulfuric acid vapor are in reasonable agreement with S_{crit} for combustion particles emitted by the jet engine operating on a fuel with high sulfur content [*Gysel et al.*, 2003; *Hitzenberger et al.*, 2003]. H_2SO_4-coated soot particles produced in our experiments have S_c in the range 0.1–1.2%, which is within the measured cloud supersaturations that can reach up to 2% [*Pruppacher and Klett*, 1997]. As shown in Figure 10, heavily coated soot particles larger than 100 nm and lightly coated soot particles larger than 300 nm have critical supersaturations lower than 0.2% [*Pierce et al.*, 2007] and hence can readily activate under typical cloud conditions.

3.3.2. Soot Coating by Sulfuric Acid in the Atmosphere

[44] In the present experiments, the flame soot particles were exposed to H_2SO_4 by passing the aerosol through a reservoir filled with 86 and 96 wt % sulfuric acid solutions at room temperature and low relative humidity (RH < 0.5%). The residence time of the soot-laden flow in the reservoir is estimated to be about 12 s. The employed vapor concentrations of H_2SO_4 are 10^9–10^{10} molecules cm^{-3} whereas the ambient vapor concentrations of sulfuric acid are significantly lower, on the order of 10^4–10^8 molecule cm^{-3} [*Eisele and McMurry*, 1997].

[45] Extrapolation of our results to atmospheric conditions requires knowledge on the relation between the coating mass fraction, gas-phase H_2SO_4 concentration, the exposure time, and the H_2SO_4 coating mechanism. As reported in our separate papers [*Pagels et al.*, 2009; *Zhang et al.*, 2008], flame soot particles subjected to sulfuric acid vapor and subsequent heating change their morphology but recover the initial mass (1.01 ± 0.04), indicating negligible chemical interaction between sulfuric acid and the particle surface. In a recent study of airborne soot particles exposed to sulfuric acid vapor, *Zhang and Zhang* [2005] using infrared spectroscopy of coated particles have arrived at a similar conclusion. The efficient formation of H_2SO_4 coating on soot and PSL particles is explained by the sticky nature of sulfuric acid and its high affinity for water [*Zhang et al.*, 1993a, 1993b]. Sulfuric acid readily condenses on particles and is subsequently stabilized from the interaction with water vapor. Absorption of water by the H_2SO_4 coating lowers the

saturation vapor pressure of H_2SO_4, resulting in practically irreversible condensation of sulfuric acid under typical atmospheric conditions.

[46] For condensation of vapor on particle surface, the effects of H_2SO_4 concentration and exposure time on the condensed mass are related inversely. Since the mass transfer rate is similar for spherical and agglomerated particles of the same mobility size [*Rogak et al.*, 1991], the condensed H_2SO_4 mass is roughly independent of the particle shape and linearly proportional to H_2SO_4 concentration. Indeed, as shown in Table 1, soot aggregates and PSL spheres of the same mobility size acquire almost identical mass of sulfuric acid. We find that increasing the concentration of gas-phase sulfuric acid by a factor of 5.6 results in a 4.6 ± 0.5 fold increase of the condensed H_2SO_4 mass. Hence, the mass of coating scales linearly with gas-phase sulfuric acid concentration. Assuming a typical daytime H_2SO_4 concentration of 10^7 molecule cm^{-3}, we estimate that achieving a coating characteristic of our present experiments requires less than 5 h. Even upon exposure to 10^5 molecule cm^{-3} sulfuric acid, a period of about 3 days is sufficient for soot particles to acquire $\sim$10% H_2SO_4 by mass and become hygroscopic. Hygroscopicity and cloud-forming potential of soot aerosols hence are considerably altered during soot typical atmospheric lifetimes of about 1 week [*Jacobson*, 2000]. Our estimates are in good agreement with the results of a recent modeling study, where for daytime conditions during summer, condensation of sulfuric acid was found to be a dominant aging process occurring on a timescale from 2 to 8 h, depending on the distance to the source region [*Riemer et al.*, 2004].

[47] It should be pointed out that certain organic species, which are produced when primary volatile organic compounds are photochemically oxidized in the presence of nitrogen oxides [*Suh et al.*, 2003; *Zhang et al.*, 2003, 2004b; *Zhao et al.*, 2004], can also condense or engage in heterogeneous reactions on soot particles [*Levitt et al.*, 2007; *Zhao et al.*, 2005, 2006]. However, it is likely that internal mixing with sulfuric acid represents the dominant process to enhance the hygroscopicity of soot in the atmosphere.

4. Conclusions

[48] In the present work the hygroscopicity of soot-containing aerosols is evaluated by simultaneously measuring the mobility and mass growth factors at relative humidities ranging from 5 to 90% using the combined tandem differential mobility analyzer (TDMA) and differential mobility analyzer–aerosol particle mass analyzer (DMA-APM) technique. Monodisperse fresh soot particles are exposed to a known concentration of sulfuric acid vapor to mimic internal mixing in the atmosphere, producing soot with a known mixing state and H_2SO_4 mass fraction. The coated particles are subjected to elevated humidity environment and the changes in their mobility diameter and mass are determined. The measured hygroscopicity is used to calculate the critical supersaturation required for coated soot particles to activate to cloud droplets.

[49] Fresh soot exhibits no hygroscopic growth at subsaturated conditions whereas soot exposed to gaseous sulfuric acid (10^9–10^{10} molecule cm^{-3}) experiences significant mobility size changes with increasing RH. Upon humidification, H_2SO_4-coated soot agglomerates display distinct hygroscopic growth patterns depending on their initial size and the mass fraction of condensed sulfuric acid. While small particles experience an increase in their mobility sizes, larger particles exhibit a marked shrinkage because of the shape change and compaction. The DMA-APM measurements reveal that particles of all sizes gain mass with increasing RH because of absorption of water by sulfuric acid coating.

[50] Freshly emitted soot particles are hydrophobic, but aging in the atmosphere increases soot hygroscopicity. Internal mixing with sulfuric acid, produced from combustion of sulfur-containing fuels and other atmospheric chemical processes, represents an important aging pathway. Our experimental results indicate that fresh soot particles upon exposure to gaseous H_2SO_4 develop a significant fraction of sulfuric acid coating and become strongly hygroscopic at subsaturated conditions, profoundly impacting their optical and cloud-forming properties. The hydrophilic soot particles are easily scavenged by cloud droplets, leading to an efficient wet removal and a reduced atmospheric lifetime of soot. The variation in the size of hygroscopic soot particles during atmospheric processing also influences deposition on the human respiratory system.

[51] Soot aggregates and polystyrene latex spheres of the same mobility size exposed to sulfuric acid vapor acquire about the same mass of condensed H_2SO_4, indicating that the coating mechanism is independent of the particle chemical composition and microphysical structure. Thus, internal mixing with sulfuric acid through H_2SO_4 vapor condensation likely represents a common aging process for a variety of atmospheric aerosols.

[52] Finally, our results suggest that the morphology, mixing state, and hygroscopicity of soot particles cannot be uniquely determined using TDMA alone during atmospheric aging, because of restructuring and filling of the voids in the soot agglomerates. A combined size and mass measurement is required to precisely quantify these properties for atmospheric soot aerosols.

[53] **Acknowledgments.** This work was supported by the U.S. Department of Energy National Institute for Climate Change Research (DOE-NICCR) and Robert A. Welch Foundation. R. Z. acknowledged additional support from National Natural Science Foundation of China Grant (40728006). J.P. was supported by a postdoctoral stipend from FORMAS, the Swedish Research Council for Environment, Agricultural Sciences and Spatial Planning. P.H.M. was supported by an NSF grant (BES-0646507).

References

Ammann, M., M. Kalberer, D. T. Jost, L. Tobler, E. Rossler, D. Piguet, H. W. Gaggeler, and U. Baltensperger (1998), Heterogeneous production of nitrous acid on soot in polluted air masses, *Nature*, *395*, 157–160, doi:10.1038/25965.

Andreae, M. O., and D. Rosenfeld (2008), Aerosol-cloud-precipitation interactions: Part 1. The nature and sources of cloud-active aerosols, *Earth Sci. Rev.*, *89*(1–2), 13–41, doi:10.1016/j.earscirev.2008.03.001.

Aubin, D. G., and J. P. D. Abbatt (2007), Interaction of NO2 with hydrocarbon soot: Focus on HONO yield, surface modification, and mechanism, *J. Phys. Chem. A*, *111*(28), 6263–6273, doi:10.1021/jp068884h.

Boubel, R. W., D. L. Fox, D. B. Turner, and A. C. Stern (1994), *Fundamentals of Air Pollution*, 574 pp., Academic, San Diego, Calif.

Collins, D. R., R. C. Flagan, and J. H. Seinfeld (2002), Improved inversion of scanning DMA data, *Aerosol Sci. Technol.*, *36*, 1–9, doi:10.1080/027868202753339032.

Crouzet, Y., and W. H. Marlow (1995), Calculations of the equilibrium vapour pressure of water over adhering 50–200 nm spheres, *Aerosol Sci. Technol.*, *22*, 43–59, doi:10.1080/02786829408959727.

Decesari, S., M. C. Facchini, E. Matta, M. Mircea, S. Fuzzi, A. R. Chughtai, and D. M. Smith (2002), Water soluble organic compounds formed by oxidation of soot, *Atmos. Environ.*, *36*, 1827–1832, doi:10.1016/S1352-2310(02)00141-3.

Dua, S. K., P. K. Hopke, and T. Raunemaa (1999), Hygroscopicity of diesel aerosols, *Water Air Soil Pollut.*, *112*, 247–257, doi:10.1023/A:1005070332691.

Ehara, K., C. Hagwood, and K. J. Coakley (1996), Novel method to classify aerosol particles according to their mass-to-charge ratio: Aerosol particle mass analyzer, *J. Aerosol Sci.*, *27*, 217–234, doi:10.1016/0021-8502(95)00562-5.

Eisele, F. L., and P. H. McMurry (1997), Recent progress in understanding particle nucleation and growth, *Philos. Trans. R. Soc. London, B*, *352*, 191–201, doi:10.1098/rstb.1997.0014.

Fan, F., R. Zhang, W.-K. Tao, and K. Mohr (2008), Effects of aerosol optical properties on deep convective clouds and radiative forcing, *J. Geophys. Res.*, *113*, D08209, doi:10.1029/2007JD009257.

Fortner, E. C., J. Zhao, and R. Zhang (2004), Development of ion drift-chemical ionization mass spectrometry, *Anal. Chem.*, *76*, 5436–5440, doi:10.1021/ac0493222.

Fuller, K. A., W. C. Malm, and S. M. Kreidenweis (1999), Effects of mixing on extinction by carbonaceous particles, *J. Geophys. Res.*, *104*, 15,941–15,954, doi:10.1029/1998JD100069.

Gasparini, R., R. Li, and D. R. Collins (2004), Integration of size distributions and size-resolved hygroscopicity measured during the Houston Supersite for compositional categorization of the aerosol, *Atmos. Environ.*, *38*, 3285–3303, doi:10.1016/j.atmosenv.2004.03.019.

Grose, M., H. Sakurai, J. C. Savstrom, M. R. Stolzenburg, W. Watts, C. G. Morgan, I. P. Murray, M. V. Twigg, D. B. Kittelson, and P. H. McMurry (2006), Chemical and physical properties of ultrafine diesel exhaust particles sampled downstream of a catalytic trap, *Environ. Sci. Technol.*, *40*, 5502–5507, doi:10.1021/es052267+.

Gundel, L. A., N. S. Guyotsionnest, and T. Novakov (1989), A study of the interaction of NO_2 with carbon particles, *Aerosol Sci. Technol.*, *10*, 343–351, doi:10.1080/02786828908959271.

Gysel, M., S. Nyeki, E. Weingartner, U. Baltensperger, H. Giebl, R. Hitzenberger, A. Petzold, and C. W. Wilson (2003), Properties of jet engine combustion particles during the PartEmis experiment: Hygroscopicity at subsaturated conditions, *Geophys. Res. Lett.*, *30*(11), 1566, doi:10.1029/2003GL016896.

Hagen, D. E., M. B. Tureblood, and P. D. Whitefield (1992), A field sampling of jet exhaust aerosols, *Particul. Sci. Technol.*, *10*, 53–63, doi:10.1080/02726359208906598.

Hering, S. V., S. K. Friedlander, J. J. Collins, and L. W. Richards (1979), Design and evaluation of a new low-pressure impactor: 2, *Environ. Sci. Technol.*, *13*, 184–188, doi:10.1021/es60150a009.

Hitzenberger, R., H. Giebl, A. Petzold, M. Gysel, S. Nyeki, E. Weingartner, U. Baltensperger, and C. W. Wilson (2003), Properties of jet engine combustion particles during the PartEmis experiment: Hygroscopic growth at supersaturated conditions, *Geophys. Res. Lett.*, *30*(14), 1779, doi:10.1029/2003GL017294.

Horvath, H. (1993), Atmospheric light absorption: A review, *Atmos. Environ., Part A*, *27*, 293–317.

Jacobson, M. Z. (2000), A physically-based treatment of elemental carbon optics: Implications for global direct forcing of aerosols, *Geophys. Res. Lett.*, *27*, 217–220, doi:10.1029/1999GL010968.

Jacobson, M. Z. (2001), Strong radiative heating due to the mixing state of black carbon in atmospheric aerosols, *Nature*, *409*, 695–697, doi:10.1038/35055518.

Jefferson, A., F. L. Eisele, P. J. Ziemann, R. J. Weber, J. J. Marti, and P. H. McMurry (1997), Measurements of the H_2SO_4 mass accommodation coefficient onto polydisperse aerosol, *J. Geophys. Res.*, *102*, 19,021–19,028, doi:10.1029/97JD01152.

Kasper, M., K. Siegmann, and K. Sattler (1997), Evaluation of in situ sampling probe for its accuracy in determining particle size distributions from flames, *J. Aerosol Sci.*, *28*, 1569–1578, doi:10.1016/S0021-8502(97)00031-1.

Khalizov, A. F., H. Xue, L. Wang, J. Zheng, and R. Zhang (2009), Enhanced light absorption and scattering by carbon soot aerosols internally mixed with sulfuric acid, *J. Phys. Chem. A*, *113*(6), 1066–1074, doi:10.1021≠jp807531n.

Kotzick, R., U. Panne, and R. Niessner (1997), Changes in condensation properties of ultrafine carbon particles subjected to oxidation by ozone, *J. Aerosol Sci.*, *28*, 725–735, doi:10.1016/S0021-8502(96)00471-5.

Levitt, N. P., R. Zhang, H. Xue, and J. Chen (2007), Heterogeneous chemistry of organic acids on soot surfaces, *J. Phys. Chem. A*, *111*, 4804–4814, doi:10.1021/jp0700480.

Li, G., R. Zhang, J. Fan, and X. Tie (2005), Impacts of black carbon aerosol on photolysis and ozone, *J. Geophys. Res.*, *110*, D23206, doi:10.1029/2005JD005898.

Löndahl, J., A. Massling, J. Pagels, E. Swietlicki, E. Vaclavik, and S. Loft (2007), Size-resolved respiratory-tract deposition of fine and ultrafine hydrophobic and hygroscopic aerosol particles during rest and exercise, *Inhal. Toxicol.*, *19*, 109–116, doi:10.1080/08958370601051677.

Maricq, M. M., S. J. Harris, and J. J. Szente (2003), Soot size distributions in rich premixed ethylene flames, *Combust. Flame*, *132*, 328–342, doi:10.1016/S0010-2180(02)00502-3.

McMurry, P. H., and M. R. Stolzenburg (1989), On the sensitivity of particle size to relative humidity for Los Angeles aerosols, *Atmos. Environ.*, *23*, 497–507, doi:10.1016/0004-6981(89)90593-3.

McMurry, P. H., X. Wang, K. Park, and K. Ehara (2002), The relationship between mass and mobility for atmospheric particles: A new technique for measuring particle density, *Aerosol Sci. Technol.*, *36*, 227–238, doi:10.1080/027868202753504083.

Mikhailov, E. F., S. S. Vlasenko, L. Kramer, and R. Niessner (2001), Interaction of soot aerosol particles with water droplets: Influence of surface hydrophilicity, *J. Aerosol Sci.*, *32*, 697–711, doi:10.1016/S0021-8502(00)00101-4.

Moteki, N., Y. Kondo, Y. Miyazaki, N. Takegawa, Y. Komazaki, G. Kurata, T. Shirai, D. R. Blake, T. Miyakawa, and M. Koike (2007), Evolution of mixing state of black carbon particles: Aircraft measurements over the western Pacific in March 2004, *Geophys. Res. Lett.*, *34*, L11803, doi:10.1029/2006GL028943.

Olfert, J. S., J. P. R. Symonds, and N. Collings (2007), The effective density and fractal dimension of particles emitted from a light-duty diesel vehicle with a diesel oxidation catalyst, *J. Aerosol Sci.*, *38*, 69–82, doi:10.1016/j.jaerosci.2006.10.002.

Pagels, J., A. F. Khalizov, P. H. McMurry, and R. Y. Zhang (2009), Processing of soot by controlled sulfuric acid and water condensation: Mass and mobility relationship, *Aerosol Sci. Technol.*, in press.

Park, K., F. Cao, D. B. Kittelson, and P. H. McMurry (2003), Relationship between particle mass and mobility for diesel exhaust particles, *Environ. Sci. Technol.*, *37*, 577–583, doi:10.1021/es025960v.

Park, K., D. B. Kittelson, M. R. Zachariah, and P. H. McMurry (2004), Measurement of inherent material density of nanoparticle agglomerates, *J. Nanopart. Res.*, *6*, 267–272, doi:10.1023/B:NANO.0000034657.71309.e6.

Perry, R. H., and D. W. Green (1997), *Perry's Chemical Engineers' Handbook*, 7th ed., 2640 pp., McGraw-Hill, New York.

Petzold, A., M. Gysel, X. Vancassel, R. Hitzenberger, H. Puxbaum, S. Vrochticky, E. Weingartner, U. Baltensperger, and P. Mirabel (2005), On the effects of organic matter and sulphur-containing compounds on the CCN activation of combustion particles, *Atmos. Chem. Phys.*, *5*, 3187–3203.

Pierce, J. R., K. Chen, and P. J. Adams (2007), Contribution of primary carbonaceous aerosol to cloud condensation nuclei: Processes and uncertainties evaluated with a global aerosol microphysics model, *Atmos. Chem. Phys.*, *7*(20), 5447–5466.

Pitchford, M., J. G. Hudson, and J. Hallet (1991), Size and critical supersaturation for condensation of jet engine exhaust particles, *J. Geophys. Res.*, *96*, 20,787–20,793, doi:10.1029/91JD02190.

Pruppacher, H. R., and J. D. Klett (1997), *Microphysics of Clouds and Precipitation*, 954 pp., Springer, New York.

Rader, D. J., and P. H. McMurry (1986), Application of the tandem differential mobility analyzer to studies of droplet growth or evaporation, *J. Aerosol Sci.*, *17*, 771–787, doi:10.1016/0021-8502(86)90031-5.

Riemer, N., H. Vogel, and B. Vogel (2004), Soot aging time scales in polluted regions during day and night, *Atmos. Chem. Phys.*, *4*, 1885–1893.

Rissler, J., J. Pagels, E. Swietlicki, A. Wierzbicka, M. Strand, L. Lillieblad, M. Sanati, and M. Bohgard (2005), Hygroscopic behavior of aerosol particles emitted from biomass fired grate boilers, *Aerosol Sci. Technol.*, *39*, 919–930, doi:10.1080/02786820500331068.

Rogak, S. N., U. Baltensperger, and R. C. Flagan (1991), Measurement of mass-transfer to agglomerate aerosols, *Aerosol Sci. Technol.*, *14*, 447–458, doi:10.1080/02786829108959505.

Saathoff, H., K.-H. Naumann, M. Schnaiter, W. Schöck, O. Möhler, U. Schurath, E. Weingartner, M. Gysel, and U. Baltensperger (2003), Coating of soot and $(NH_4)_2SO_4$ particles by ozonolysis products of α-pinene, *J. Aerosol Sci.*, *34*, 1297–1321, doi:10.1016/S0021-8502(03)00364-1.

Sakurai, H., K. Park, P. H. McMurry, D. D. Zarling, D. B. Kittelson, and P. J. Ziemann (2003a), Size-dependent mixing characteristics of volatile and nonvolatile components in diesel exhaust aerosols, *Environ. Sci. Technol.*, *37*, 5487–5495, doi:10.1021/es034362t.

Sakurai, H., H. J. Tobias, K. Park, D. Zarling, S. Docherty, D. B. Kittelson, P. H. McMurry, and P. J. Ziemann (2003b), On-line measurements of diesel nanoparticle composition and volatility, *Atmos. Environ.*, *37*, 1199–1210, doi:10.1016/S1352-2310(02)01017-8.

Santoro, R. J., H. G. Semerjian, and R. A. Dobbins (1983), Soot particle measurements in diffusion flames, *Combust. Flame*, *51*, 203–218, doi:10.1016/0010-2180(83)90099-8.

Seinfeld, J. H., and S. N. Pandis (1998), *Atmospheric Chemistry and Physics: From Air Pollution to Climate Change*, 1326 pp., John Wiley, New York.

Shi, Z. B., D. Z. Zhang, H. Z. Ji, S. Hasegawa, and M. Hayashi (2008), Modification of soot by volatile species in an urban atmosphere, *Sci. Total Environ.*, *389*(1), 195–201, doi:10.1016/j.scitotenv.2007.08.016.

Shiraiwa, M., Y. Kondo, N. Moteki, N. Takegawa, Y. Miyazaki, and D. R. Blake (2007), Evolution of mixing state of black carbon in polluted air from Tokyo, *Geophys. Res. Lett.*, *34*, L16803, doi:10.1029/2007GL029819.

Suh, I., R. Zhang, L. T. Molina, and M. J. Molina (2003), Oxidation mechanism of aromatic peroxy and bicyclic radicals from OH-toluene reactions, *J. Am. Chem. Soc.*, *125*, 12,655–12,665, doi:10.1021/ja0350280.

Swietlicki, E., et al. (2008), Hygroscopic properties of submicrometer atmospheric aerosol particles measured with H-TDMA instruments in various environments: A review, *Tellus, Ser. B*, *60*, 432–469.

Viggiano, A. A., J. V. Seeley, P. L. Mundis, J. S. Williamson, and R. A. Morris (1997), Rate constants for the reactions of $XO_3^-(H2O)_{(n)}$ (X = C, HC, and N) and $NO_3^-(HNO_3)_{(n)}$ with H_2SO_4: Implications for atmospheric detection of H_2SO_4, *J. Phys. Chem. A*, *101*, 8275–8278, doi:10.1021/jp971768h.

Wang, S. C., and R. C. Flagan (1990), Scanning electrical mobility spectrometer, *Aerosol Sci. Technol.*, *13*, 230–240, doi:10.1080/02786829008959441.

Weingartner, E., U. Baltensperger, and H. Burtscher (1995), Growth and structural change of combustion aerosols at high relative humidity, *Environ. Sci. Technol.*, *29*, 2982–2986, doi:10.1021/es00012a014.

Weingartner, E., H. Burtscher, and U. Baltensperger (1997), Hygroscopic properties of carbon and diesel soot particles, *Atmos. Environ.*, *31*, 2311–2327, doi:10.1016/S1352-2310(97)00023-X.

Widmann, J. F., J. C. Yang, T. J. Smith, S. L. Manzello, and G. W. Mulholland (2003), Measurement of the optical extinction coefficients of post-flame soot in the infrared, *Combust. Flame*, *134*, 119–129, doi:10.1016/S0010-2180(03)00089-0.

Wyslouzil, B. E., K. L. Carleton, D. M. Sonnenfroh, W. T. Rawlins, and S. Arnold (1994), Observation of hydration of single, modified carbon aerosols, *Geophys. Res. Lett.*, *21*, 2107–2110, doi:10.1029/94GL01588.

Zhang, D., and R. Zhang (2005), Laboratory investigation of heterogeneous interaction of sulfuric acid with soot, *Environ. Sci. Technol.*, *39*, 5722–5728, doi:10.1021/es050372d.

Zhang, R., P. J. Wooldridge, J. P. D. Abbatt, and M. J. Molina (1993a), Physical chemistry of the H_2SO_4/H_2O binary system at low temperatures: Implications for the stratosphere, *J. Phys. Chem.*, *97*, 7351–7358, doi:10.1021/j100130a038.

Zhang, R., P. J. Wooldridge, and M. J. Molina (1993b), Vapor pressure measurements for the $H_2SO_4/HNO_3/H_2O$ and $H_2SO_4/HCl/H_2O$ systems: Incorporation of stratospheric acids into background sulfate aerosols, *J. Phys. Chem.*, *97*, 8541–8548, doi:10.1021/j100134a026.

Zhang, R., X. Tie, and D. W. Bond (2003), Impacts of anthropogenic and natural NO_x sources over the U. S. on tropospheric chemistry, *Proc. Natl. Acad. Sci. U. S. A.*, *100*, 1505–1509, doi:10.1073≠pnas.252763799.

Zhang, R., I. Suh, J. Zhao, D. Zhang, E. C. Fortner, X. X. Tie, L. T. Molina, and M. J. Molina (2004a), Atmospheric new particle formation enhanced by organic acids, *Science*, *304*, 1487–1490, doi:10.1126/science.1095139.

Zhang, R., W. Lei, X. Tie, and P. Hess (2004b), Industrial emissions cause extreme diurnal urban ozone variability, *Proc. Natl. Acad. Sci. U. S. A.*, *101*, 6346–6350, doi:10.1073≠pnas.0401484101.

Zhang, R., A. F. Khalizov, J. Pagels, D. Zhang, H. Xue, and P. H. McMurry (2008), Variability in morphology, hygroscopicity and optical properties of soot aerosols during atmospheric processing, *Proc. Natl. Acad. Sci. U. S. A.*, *105*, 10,291–10,296, doi:10.1073/pnas.0804860105.

Zhao, J., R. Zhang, E. C. Fortner, and S. W. North (2004), Quantification of hydroxycarbonyls from OH-isoprene reactions, *J. Am. Chem. Soc.*, *126*, 2686–2687, doi:10.1021/ja0386391.

Zhao, J., N. P. Levitt, and R. Zhang (2005), Heterogeneous chemistry of octanal and 2, 4-hexadienal with sulfuric acid, *Geophys. Res. Lett.*, *32*, L09802, doi:10.1029/2004GL022200.

Zhao, J., N. P. Levitt, R. Zhang, and J. Chen (2006), Heterogeneous reactions of methylglyoxal in acidic media: Implications for secondary organic aerosol formation, *Environ. Sci. Technol.*, *40*, 7682–7687, doi:10.1021/es060610k.

Zuberi, B., K. S. Johnson, G. K. Aleks, L. T. Molina, M. J. Molina, and A. Laskin (2005), Hydrophilic properties of aged soot, *Geophys. Res. Lett.*, *32*, L01807, doi:10.1029/2004GL021496.

A. F. Khalizov, H. Xue, D. Zhang, and R. Zhang, Department of Atmospheric Sciences, Texas A&M University, College Station, TX 77843, USA. (zhang@ariel.met.tamu.edu)

P. H. McMurry and J. Pagels, Department of Mechanical Engineering, University of Minnesota, Minneapolis, MN 55455, USA.